

Off-shell persistence of composite pions and kaons

Si-Xue Qin,^{1,*} Chen Chen,^{2,†} Cédric Mezrag,^{3,‡} and Craig D. Roberts^{3,§}

¹*Department of Physics, Chongqing University, Chongqing 401331, People's Republic of China*

²*Instituto de Física Teórica, Universidade Estadual Paulista, 01140-070 São Paulo, Brazil*

³*Physics Division, Argonne National Laboratory, Argonne, Illinois 60439, USA*



(Received 20 February 2017; revised manuscript received 20 November 2017; published 17 January 2018)

In order for a Sullivan-like process to provide reliable access to a meson target as t becomes spacelike, the pole associated with that meson should remain the dominant feature of the quark-antiquark scattering matrix and the wave function describing the related correlation must evolve slowly and smoothly. Using continuum methods for the strong-interaction bound-state problem, we explore and delineate the circumstances under which these conditions are satisfied: for the pion, this requires $-t \lesssim 0.6 \text{ GeV}^2$, whereas $-t \lesssim 0.9 \text{ GeV}^2$ will suffice for the kaon. These results should prove useful in planning and evaluating the potential of numerous experiments at existing and proposed facilities.

DOI: [10.1103/PhysRevC.97.015203](https://doi.org/10.1103/PhysRevC.97.015203)

I. INTRODUCTION

The notion that a nucleon possesses a meson cloud is not new [1]. In effect, this feature is kindred to the dressing of an electron by virtual photons in quantum electrodynamics [2] or the existence of dressed quarks with a running mass generated by a cloud of gluons in quantum chromodynamics (QCD) [3–7]. Naturally, any statement that each nucleon is accompanied by a meson cloud is only meaningful if observable consequences can be derived therefrom. A first such suggestion is canvassed in Ref. [8], which indicates, e.g., that a calculable fraction of the nucleon's antiquark distribution is generated by its meson cloud. Mirroring this effect, one may argue that a nucleon's meson cloud can be exploited as a target and thus, for instance, the so-called Sullivan processes can provide a means by which to gain access to the pion's elastic electromagnetic form factor [9–13], Fig. 1(a), and also its valence-quark parton distribution functions (PDFs) [14–16], Fig. 1(b).

One issue in using the Sullivan process as a tool for accessing a “pion target” is that the mesons in a nucleon's cloud are virtual (off-shell) particles. This concept is readily understood when such particles are elementary fields, e.g., photons, quarks, gluons. However, providing a unique definition of an off-shell bound state in quantum field theory is problematic.

Physically, for both form factor and PDF extractions, $t < 0$ in Fig. 1, so the total momentum of the π^* is spacelike.¹ Therefore, in order to maximize the true-pion content in any measurement, kinematic configurations are chosen in order to minimize $|-t|$. This is necessary but not sufficient to

ensure the data obtained thereby are representative of the physical pion. Additional procedures are needed in order to suppress nonresonant (nonpion) background contributions; and modern experiments and proposals make excellent use of, e.g., longitudinal-transverse cross-section separation and low-momentum tagging of the outgoing nucleon.

Notwithstanding their ingenuity, such experimental techniques cannot directly address the following question: supposing it is sensible to speak of an off-shell pion with total momentum P , where $P^2 = (v-1)m_\pi^2$, $m_\pi \approx 0.14 \text{ GeV}$, so that $v \geq 0$ defines the pion's virtuality, then how do the qualities of this system depend on v ? If the sensitivity is weak, then $\pi^*(v)$ is a good surrogate for the physical pion; but if the distributions of, e.g., charge or partons, change significantly with v , then the processes in Fig. 1 can reveal little about the physical pion. Instead, they express features of the entire compound reaction. Since there is no unique definition of an off-shell bound state, the question we have posed does not have a precise answer. On the other hand, one can use the bound-state equations of continuum quantum field theory in order to explore the issue.

II. PIONS: ON- AND OFF-SHELL

All correlations with pion-like quantum numbers, both resonant and continuum, are accessible via the inhomogeneous pseudoscalar Bethe-Salpeter equation

$$\Gamma_5(k; P) = Z_4 \gamma_5 + \int_{dq}^\Lambda [\chi_5(q; P)]_{sr} K_{tu}^{rs}(q, k; P), \quad (1)$$

where $\chi_5(q; P) = S(q_\eta) \Gamma_5(q; P) S(q_{\bar{\eta}})$, $q_\eta = q + \eta P$, $q_{\bar{\eta}} = q - (1 - \eta)P$, P is the total quark-antiquark momentum; \int_{dq}^Λ represents a Poincaré invariant regularization of the four-dimensional integral, with Λ the regularization mass scale; and $Z_4(\zeta^2, \Lambda^2)$ is the mass renormalization constant, with ζ the renormalization point. In addition, S is the dressed propagator for a u or d quark (we assume isospin symmetry throughout), K

*sqin@cqu.edu.cn

†chenchen@ift.unesp.br

‡cedric.mezrag@roma1.infn.it

§cdroberts@anl.gov

¹We use a Euclidean metric: $\{\gamma_\mu, \gamma_\nu\} = 2\delta_{\mu\nu}$; $\gamma_5 = \gamma_4 \gamma_1 \gamma_2 \gamma_3$, $\text{tr}[\gamma_5 \gamma_\mu \gamma_\nu \gamma_\rho \gamma_\sigma] = -4\epsilon_{\mu\nu\rho\sigma}$; $\sigma_{\mu\nu} = (i/2)[\gamma_\mu, \gamma_\nu]$; $a \cdot b = \sum_{i=1}^4 a_i b_i$; and P_μ spacelike $\Rightarrow P^2 > 0$.

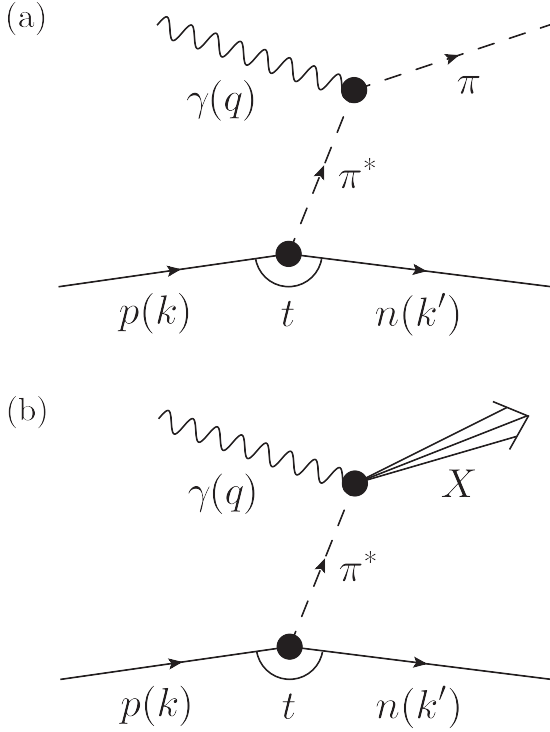


FIG. 1. Sullivan processes, in which a nucleon’s pion cloud is used to provide access to the pion’s (a) elastic form factor and (b) parton distribution functions. $t = -(k - k')^2$ is a Mandelstam variable and the intermediate pion, $\pi^*(P = k - k')$, $P^2 = -t$, is off-shell.

is the quark-antiquark scattering kernel, and the indices r, s, t, u denote the matrix structure of the elements in the equation.

The physical ($v = 0$) pion appears as a pole in the pseudoscalar vertex, viz. [17]

$$\Gamma_5(k; P) \stackrel{P^2 + m_\pi^2 \simeq 0}{=} \frac{\rho_\pi^\xi}{P^2 + m_\pi^2} \Gamma_\pi(k; P) + \text{reg.}, \quad (2)$$

where “reg.” denotes terms analytic on $\nu m_\pi^2 \simeq 0$,

$$\begin{aligned} \Gamma_\pi(k; P) = & \gamma_5 [i E_\pi(k; P) + \gamma \cdot P F_\pi(k; P) \\ & + \gamma \cdot k k \cdot P G_\pi(k; P) + \sigma_{\mu\nu} k_\mu P_\nu H_\pi(k; P)] \end{aligned} \quad (3)$$

is the pion’s Bethe-Salpeter amplitude and ρ_π^ξ measures the ratio of the in-pion condensate and the pion’s leptonic decay constant [18].

In proposing reactions like those in Fig. 1 as paths to real-pion targets, one is naively thought to assume that for some nonzero and sizable v_S , the pion pole remains the dominant feature of the pseudoscalar vertex and the pion’s wave function is “frozen”:

$$\Gamma_5(k; P) \stackrel{v < v_S}{\approx} \frac{\rho_\pi^\xi}{P^2 + m_\pi^2} \Gamma_\pi(k; P). \quad (4)$$

With modern methods of experiment and analysis, however, the reactions in Fig. 1 provide sound realizations of a pion target under softer assumptions; namely, the pole associated with the ground-state pion remains the dominant feature of

the vertex (equivalently, the quark-antiquark scattering matrix) and the Bethe-Salpeter-like amplitude describing the related correlation evolves slowly and smoothly with virtuality. Under these conditions, then $\forall v < v_S$ a judicious extrapolation of a cross section to $v = 0$ will yield a valid estimate of the desired on-shell result. The question posed in the Introduction may now be translated into the challenge of determining the value of v_S for which these conditions are satisfied.

To address this issue, we consider the following modified Bethe-Salpeter equation:

$$\Gamma_5(k; P) = Z_4 \gamma_5 + \lambda(v) \int_{dq}^\Lambda [\chi_5(q; P)]_{sr} K_{tu}^{rs}(q, k; P), \quad (5)$$

introduced about 50 years ago and discussed extensively in Ref. [19]. Importantly, since the equation determining the residue of any pole-solution to Eq. (5), i.e., the related homogeneous Bethe-Salpeter equation, is the same in any channel that possesses overlap with the pion, then for the purpose of elucidating the character of an off-shell pion, it suffices to consider Eq. (5).

$\lambda(v)$ in Eq. (5) may be interpreted as a coupling, upon which, *inter alia*, the nature and location of all pole solutions to this equation depend. The original Bethe-Salpeter equation, Eq. (1), is recovered when $\lambda(v=0) = 1$, at which point the canonical normalization of the bound-state amplitude is fixed by enforcing a constraint on $d\lambda(v)/dv|_{v=0}$. If $\lambda(v)$ is shifted to values below unity, i.e., the coupling is weakened, then the $(-P^2)$ location (bound-state mass-squared) of the first pole solution, Eq. (2), moves to larger values: the ground-state “pion” becomes heavier. On the other hand, if $\lambda(v)$ is increased above unity, then the first pole-solution moves to $v > 0$, viz. the pseudopion becomes lighter and, eventually, the pole solution shifts to spacelike momenta. Owing to linearity, Eq. (5) evidently defines a class of solutions for $\Gamma_5(k; P)$ that depend smoothly on $\lambda(v)$, and all such solutions have the property

$$\Gamma_5(k; P|\lambda(v)) \stackrel{P^2 + (1-v)m_\pi^2 \simeq 0}{=} \frac{\rho_\pi^\xi(v)}{P^2 + (1-v)m_\pi^2} \Gamma_\pi(k; P|\lambda(v)) + \text{reg.}, \quad (6)$$

namely, in the neighborhood of the pseudopion pole, the vertex is effectively represented by a free-particle propagator for that state with a residue proportional to its Bethe-Salpeter amplitude. This is the desired generalization of Eq. (4).

It is now apparent that within the context of the continuum bound-state problem in quantum field theory, Eq. (5) provides the natural framework for analyses of the virtuality dependence of pion properties.² Indeed, in one way or another, this equation and the smooth virtuality dependence of the solutions, $\Gamma_5(k; P; \lambda(v))$, are an integral part of every continuum study of the bound-state problem in QCD, with off-shell calculations

²Off-shell mesons are typically defined more simply [20–27]. For example, in Refs. [23–27] the internal structure is assumed to be frozen and off-shell features, when incorporated, are expressed solely through the virtuality dependence of a vacuum polarization diagram built using the frozen amplitudes. Our framework delivers a unification and generalization of these approaches.

leading to (verified or verifiable) on-shell predictions (e.g., Refs. [28–37]). In this connection, the quantity $\delta(v) := [\lambda(v) - 1]$ can be said to measure deviations induced by nonzero pion virtuality. Equation (6) states that at any value of $P^2 = (v-1)m_\pi^2$, there is a unique value $\lambda(v)$ for which Eq. (5) exhibits an (off-shell) pion pole at $(v-1)m_\pi^2$. Subsequently, a comparison between the Bethe-Salpeter amplitude obtained at that pole and the $v=0$ amplitude will reveal the nature of (any) changes in the internal structure of the associated correlation; and the same result is obtained irrespective of the particular interpolating field used to generate an overlap with the pion. The value of v_S is the boundary of the v domain for which any such modifications are modest. Here, “modest” means that all quantitative measures of structural change evolve slowly and smoothly with v .

III. COMPUTED PROPERTIES OF AN OFF-SHELL PION

The character of an off-shell pion may be assessed by any nonperturbative approach that provides access to the solution of Eq. (5) because, as we have highlighted above, all bound-state equations with a connection to the pion channel possess identical structure at the pole, wherever it is located, and the form of Eq. (5) makes no assumptions about the character of the Bethe-Salpeter kernel. In order to proceed, we choose to approach this problem using methods developed for the continuum bound-state problem [38–41].

The kernel of Eq. (5) involves the dressed light-quark propagators, so it is coupled with the light-quark gap equation. The problem can therefore be analysed by using a symmetry-preserving truncation of this pair of equations. A systematic scheme is described in Refs. [42–44]; and the leading-order term is the widely used rainbow-ladder (RL) truncation. It is known to be capable of delivering a good description of π and K mesons [38–41], for example, because corrections in these channels largely cancel owing to the preservation of relevant Ward-Green-Takahashi identities.

A more realistic description is provided by the class of symmetry-preserving DB kernels [45], i.e., dynamical chiral symmetry breaking (DCSB) improved kernels, which shrink the gap between nonperturbative continuum-QCD and the *ab initio* prediction of bound-state properties [46–48]. A basic difference between the two is that DB kernels produce a smoother transition between the weak- and strong-coupling domains of QCD, something that is expressed in mesons, e.g., via softer leading-twist parton distribution amplitudes (PDAs) [49–51]. Having made the distinctions clear, we now note that the RL truncation is adequate herein because we aim to explore contrasts between bound-state properties off- and on-shell, and differences between RL and DB results will largely cancel in such ratios.

In RL truncation, the relevant gap- and Bethe-Salpeter equations are $[p = k - q, T_{\mu\nu}(p) = \delta_{\mu\nu} - p_\mu p_\nu / p^2]$ [52–54]:

$$S^{-1}(k) = Z_2 (i\gamma \cdot k + m^{\text{bm}}) + \Sigma(k), \quad (7a)$$

$$\Sigma(k) = Z_2^2 \int_{dq}^{\Lambda} \bar{G}(p^2) T_{\mu\nu}(p) \frac{\lambda^a}{2} \gamma_\mu S(q) \frac{\lambda^a}{2} \gamma_\nu, \quad (7b)$$

where Z_2 is the quark wave function renormalization; and

$$\Gamma_5(k; P) = Z_4 \gamma_5 - \lambda(v) Z_2^2 \times \int_{dq}^{\Lambda} \bar{G}(p^2) T_{\mu\nu}(p) \frac{\lambda^a}{2} \gamma_\mu \chi_5(q; P) \frac{\lambda^a}{2} \gamma_\nu. \quad (8)$$

Equations (7), (8) are complete once the process-independent running interaction is specified; and we use [54,55]

$$\bar{G}(s) = \frac{8\pi^2}{\omega^5} \zeta^3 e^{-s/\omega^2} + \frac{8\pi^2 \gamma_m \mathcal{F}(s)}{\ln[\tau + (1 + s/\Lambda_{\text{QCD}}^2)^2]}, \quad (9)$$

where $\gamma_m = 12/25$, $\Lambda_{\text{QCD}} = 0.234$ GeV; $\tau = e^2 - 1$; $\mathcal{F}(s) = \{1 - \exp(-s/[4m_t^2])\}/s$, $m_t = 0.5$ GeV; $\zeta = 0.8$ GeV, $\omega = m_t$; and a renormalization scale $\zeta = \zeta_{19} = 19$ GeV [52]. The connection between Eq. (9) and QCD’s gauge sector is canvassed elsewhere [46–48]. Here we only note that Eq. (9) has the correct shape but is too large in the infrared, for reasons that are well understood. Notwithstanding this, used judiciously in RL truncation, Eq. (9) serves as a valuable tool for hadron physics phenomenology. (Notably, for a wide range of observables, Eq. (9) produces results that are practically equivalent to those computed using earlier parametrizations [52,56].)

Solving Eq. (7) for the dressed propagator, $S(k) = 1/[i\gamma \cdot k A(k^2) + B(k^2)]$, is now straightforward; and, with the solution in hand, the kernel of Eq. (8) is fully determined. Thus, using $m^{\zeta_{19}} = 3.4$ MeV, at the on-shell point, $\lambda(v=0) = 1$, we obtain [55]: $m_\pi = 0.134$ GeV, $f_\pi = 0.093$ GeV in fair agreement with experiment [57].

With this foundation, we can begin to explore the persistence of pionic characteristics as one takes the correlation off-shell. To that end, in Fig. 2 (upper panel) we depict the v dependence of the virtuality eigenvalue: the result is linear on $v \lesssim 45$,

$$\lambda(v) = 1 + 0.016 v, \quad (10)$$

i.e., the change in $\lambda(v)$ is purely kinematic and, hence, the pion pole dominates the quark-antiquark scattering kernel $\forall v < 45$.

The next issue to address is if/how the internal structure of the correlation is modified. A detailed picture of possible rearrangements of the pion’s internal structure can be obtained by studying the impact of $v > 0$ on the scalar functions in Eq. (3). This is illustrated in Fig. 2 (lower panel), which depicts the k^2 dependence of the ratio of the leading Chebyshev moment for one of the ultraviolet (UV) dominant amplitudes in Eq. (3), where for any function that leading moment is $(x = k \cdot P / \sqrt{k^2 P^2})$

$$\mathcal{M}(k^2; P^2) = \frac{2}{\pi} \int_{-1}^1 dx \sqrt{1-x^2} \mathcal{M}(k^2, x; P^2). \quad (11)$$

The evolution pattern of the correlation’s internal structure is more subtle than that of $\lambda(v)$. Notwithstanding that, we find that structural modifications are significant $\forall v > 45$. Moreover, there is a measure of ambiguity in demarcating the domain within which structural changes can be considered modest. We therefore choose conservatively and identify $v_S \approx 31$, since on the domain $v \lesssim v_S$ the pattern exhibited by the ratios in Fig. 2 is both simple and readily interpreted. Namely,

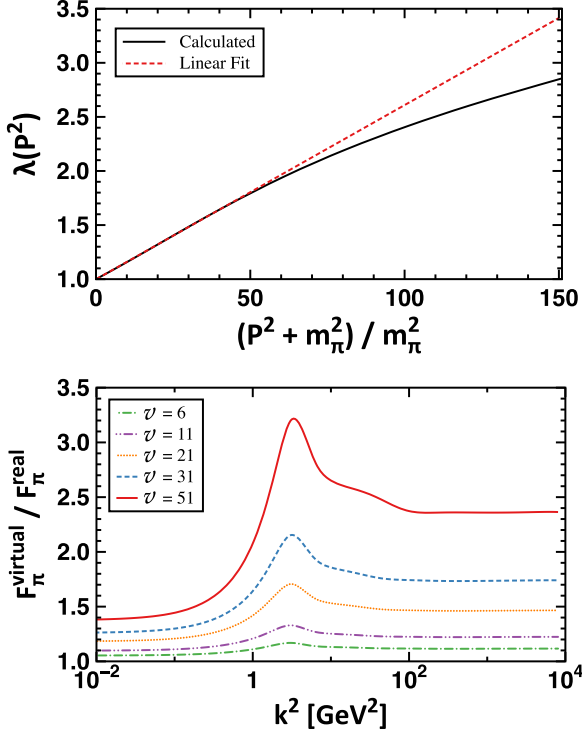


FIG. 2. Upper panel: v dependence of the virtuality eigenvalue introduced in Eq. (5). The curve is linear on $v \lesssim 45$, Eq. (10), a result which indicates that the pion pole dominates the quark-antiquark scattering kernel on this domain. Lower panel: v dependence exhibited by one of the UV-dominant terms in the pion's Bethe-Salpeter amplitude, Eq. (3).

on $k^2 \lesssim 1 \text{ GeV}^2$, i.e., at length scales $\ell_\pi \gtrsim 0.2 \text{ fm}$, the impact of $v \neq 0$ on the pion's internal structure is modest, even at $v = 31$. The domain $k^2 \in [1, 4] \text{ GeV}^2$ is a smooth region of transition into the UV. Then, on $k^2 \gtrsim 4 \text{ GeV}^2$, viz. for $\ell \lesssim 0.1 \text{ fm}$, one observes plateaux, which describe nearly constant shifts in the amplitudes. The magnitude of the shifts grows with v and that growth is linear to within 3.5%.

The UV tail of the pion's Bethe-Salpeter amplitude maps algebraically into a v dependence of ρ_π^ζ in Eq. (2):

$$i\rho_\pi^\zeta(v) = Z_4 \text{tr}_{\text{CD}} \int_{dq}^\Lambda \gamma_5 \chi_\pi(q^2, q \cdot P; v), \quad (12)$$

where $\chi_\pi = S(q_\eta) \Gamma_\pi(q^2, q \cdot P; v) S(q_{\bar{\eta}})$ and the trace is over color and spinor indices, because the value of the integral in Eq. (12) is determined by the ultraviolet behavior of the integrand [58]. An analogous leptonic decay constant can also be defined:

$$f_\pi(v) P_\mu = Z_4 \text{tr}_{\text{CD}} \int_{dq}^\Lambda \gamma_5 \gamma_\mu \chi_\pi(q^2, q \cdot P; v). \quad (13)$$

One can now form the product $\kappa_\pi^\zeta(v) := f_\pi(v) \rho_\pi^\zeta(v)$, which is a quark-antiquark core density for the correlation, an in-pion condensate [18], whose growth with virtuality is depicted in Fig. 3. Unsurprisingly, given the preceding observations, $\kappa_\pi^\zeta(v)$

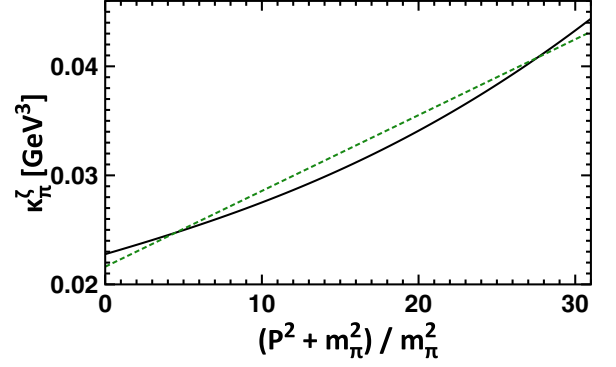


FIG. 3. Virtuality dependence of the quark-antiquark core density in the pion correlation: solid (black) curve. On the depicted domain, the evolution is linear to within 3%, as highlighted by the dashed (green) line. (We use $\zeta = 19 \text{ GeV}$.)

grows approximately linearly with virtuality on $v \lesssim v_S$:

$$\kappa_\pi^\zeta(v) \approx \kappa_\pi^\zeta(0) [1 + 0.032v], \quad \kappa_\pi^\zeta(0) = (0.28 \text{ GeV})^3. \quad (14)$$

Hence, the picture that emerges from our analysis of Eq. (5) is an off-shell pion whose internal structure is essentially unaltered at length scales $\ell_\pi \gtrsim 0.1 \text{ fm}$. On the other hand, at the core ($\ell_\pi \lesssim 0.1 \text{ fm}$) the quark-antiquark density increases slowly with virtuality, reaching a value at $v = 31$ which is roughly twice that of the on-shell pion, in line with expectations based upon the plateaux in Fig. 2. (A linear fit to $\kappa_\pi^\zeta(v)$ on $v \in [0, 55]$ is a poor representation of the result: the rms difference is greater than 10% and it underestimates $\kappa_\pi^\zeta(0)$ by 40%.)

As evident in Fig. 1, only one pion is off-shell when using the Sullivan process to generate a hadron target. Consequently, the modest structural changes described above enter linearly in the scattering amplitudes. Their impact is illustrated in Fig. 4, which depicts the $\pi^*(v) + \gamma \rightarrow \pi$ transition form factor, $F_\pi^*(Q^2, v)$. Using the “brute force” algorithm employed in Ref. [59] (to compute the propagators, Bethe-Salpeter amplitudes, photon-quark vertex, and scattering amplitude) yields the curves drawn in the upper panel of Fig. 4. Those curves terminate at $Q^2 = 4 \text{ GeV}^2$ because the algorithm is unreliable at larger momenta.

To complete the calculation of $F_\pi^*(Q^2, v)$ directly at arbitrarily large spacelike Q^2 , it would be necessary to use the method introduced in Ref. [60], i.e., develop a new perturbation theory integral representation for the Bethe-Salpeter amplitude at each required value of the virtuality. That is straightforward but time consuming, so we employ a simpler expedient. Namely, we capitalize on the analysis in Ref. [60], which shows that the computed elastic pion form factor can accurately be interpolated by a monopole multiplied by a simple factor that restores the correct QCD anomalous dimension. We therefore write

$$F_\pi^*(Q^2, v) = \frac{1}{1 + Q^2/m_0^2} \mathcal{A}(Q^2, v), \quad (15a)$$

$$\mathcal{A}(Q^2, v) = \frac{1 + Q^2 a_0^2(v)}{1 + Q^2 [a_0^2(v)/b_u^2(v)] \ln(1 + Q^2/\Lambda_{\text{QCD}}^2)}, \quad (15b)$$

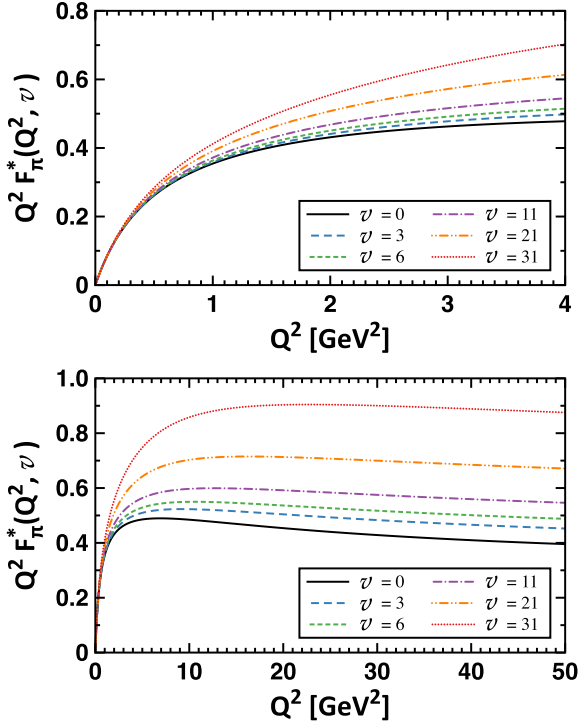


FIG. 4. Upper panel: Direct calculation of the $\pi^*(v) + \gamma \rightarrow \pi$ transition form factor at a range of virtuality values. Lower panel: Constrained extrapolations to large Q^2 using Eq. (15).

where $m_0 = 0.72$ GeV (i.e., the ρ -meson mass computed using this framework [54]) is fixed by the elastic pion form factor, and $a_0(v)$, $b_u(v)$ are fitted to the behavior of $F_\pi^*(Q^2, v)$ on $Q^2 \in [0, 4]$ GeV²:

$$a_0(v) = 0.29(1 + 0.028 v), \quad (16a)$$

$$b_u(v) = 2.3(1 + 0.017 v). \quad (16b)$$

The lower panel depicts a collection of such constrained extrapolations. Pointwise comparison with Fig. 2 in Ref. [60] demonstrates the veracity of Eq. (15) for $v = 0$.

An important feature of the transition form factor is highlighted by the lower panel of Fig. 4, viz. once again, on $v \lesssim v_s$ the magnitude of $F_\pi^*(Q^2, v)$ for $Q^2 \gtrsim 10$ GeV² grows approximately linearly with v . This, too, can be traced to the behavior illustrated in Fig. 2 (lower panel) because, reviewing the analysis in Ref. [61], it is readily established that the UV behavior of the $\pi^*(v) + \gamma \rightarrow \pi$ transition form factor must respond linearly to changes in the Bethe-Salpeter amplitude and such modifications should become evident on just this domain.

One can elaborate by recalling [62–64]

$$Q^2 F_\pi(Q^2) \stackrel{Q^2 \gg \Lambda_{\text{QCD}}^2}{\approx} 16\pi\alpha_s(Q^2) f_\pi^2 w_\phi^2, \quad (17a)$$

$$w_\phi = \frac{1}{3} \int_0^1 dx \frac{1}{x} \varphi_\pi(x), \quad (17b)$$

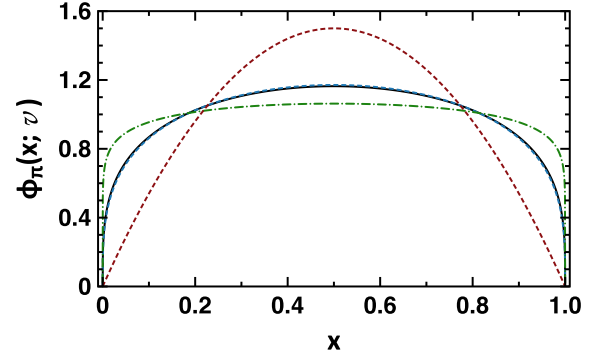


FIG. 5. Virtuality dependence of pion twist-two PDA. Solid curve: inferred $v = 0$ result, a good approximation to that calculated in RL truncation, dashed (blue) [49,60]; and dot-dashed (green) curve, inferred PDA at $v = 31$. Even this appreciable virtuality only introduces a modest rms relative-difference between the PDAs determined herein, namely, 13%. Measured equivalently, the RL result differs by 34% from that appropriate to QCD's conformal limit (dotted, red).

where $\varphi_\pi(x)$ is the pion's twist-two valence-quark PDA. Contemporary analyses demonstrate that ground-state meson PDAs are well represented by [49–51,65] $\varphi(x) = \mathcal{N}_p [x(1-x)]^p$, where \mathcal{N}_p ensures $\int_0^1 dx \varphi(x) = 1$. Moreover, when the consistently computed PDA is used, Eq. (17) underestimates the direct RL calculation by only 15% on $Q^2 \simeq 8$ GeV². One may therefore equate Eq. (17) with 85% of the UV limit of Eq. (15) and infer p . This procedure yields $p(v=0) = 0.29$, to be compared with $p = 0.30$ in Ref. [60], thereby confirming its validity and also the remark following Eqs. (16).³ For $v > 0$, Eq. (17) receives minor modifications: $f_\pi^2 \rightarrow f_\pi f_\pi(v)$ and $w_\phi^2 \rightarrow w_\phi w_\phi(v)$, where $\varphi(x; v)$ is a PDA for the off-shell pion. Using the revised formula in the matching procedure and assuming the offset remains at 15%, then $p(v=31) = 0.105$. This inferred virtuality dependence of the PDA is depicted in Fig. 5: the dilation grows modestly with increasing v . Such a connection between the UV behavior of the pion's Bethe-Salpeter amplitude and dilation of the PDA is readily verified using a simple generalisation of the algebraic model introduced in Ref. [49].

At this point, we use generalized parton distributions (GPDs) to translate the behavior of $F_\pi^*(Q^2, v)$ into insights regarding the impact of virtuality on extractions of the pion's valence-quark PDF via the process in Fig. 1(b). In particular, recall that the elastic form factor can be written [67–69]

$$F_\pi(Q^2) = \int_{-1}^1 dx H_{\pi^+}^u(x, 0, Q^2), \quad (18a)$$

$$u^\pi(x) = H_{\pi^+}^u(x > 0, 0, 0), \quad (18b)$$

where $H_{\pi^+}^u(x, 0, Q^2)$ is the pion's GPD and $u^\pi(x)$ is its valence-quark distribution function. Notably, too, at a typical hadronic

³Direct comparison is meaningful because Ref. [60] neglected evolution of the pion's Bethe-Salpeter wave function, whose role and importance is discussed in Refs. [36,66].

scale [70]

$$H_{\pi^+}^u(x, 0, Q^2) \stackrel{x \lesssim 1}{\sim} (1-x)^2 \quad \forall Q^2 < \infty. \quad (19)$$

Hence, considering a half-off-shell generalization of the GPD, which may be accomplished following Ref. [71], using a matrix element defined with an initial state corresponding to the lowest-mass pole solution of Eq. (5), and given the modest v dependence of $F_{\pi^*}(Q^2, v)$, Eqs. (18), (19) indicate that $u^\pi(x; v)$ will behave similarly. In particular, the power-law describing its decay on $x \simeq 1$ should not depend strongly on v .

IV. CONCLUSION

We have explored the properties of an off-shell pion by introducing a virtuality eigenvalue, $\lambda(v)$, into the Bethe-Salpeter equations describing the formation of bound states and correlations in scattering channels that overlap with the pion. The pion pole dominates the scattering matrix so long as $\lambda(v)$ is linear in the virtuality, v . Within this linearity domain, alterations of the pion's internal structure induced by $v > 0$ can be analyzed by charting the v dependence of the pointwise behavior of the Bethe-Salpeter amplitude describing the correlation. Following this procedure, we demonstrated that for $v \lesssim v_S = 31$, which corresponds to $-t \lesssim 0.6 \text{ GeV}^2$

in the notation of Fig. 1, the off-shell correlation serves as a valid pion target. Namely, on this domain the properties of the off-shell correlation are simply related to those of the on-shell pion and, consequently, a judicious extrapolation to $v = 0$ will deliver reliable results for pion properties.

In the present context it is natural to ask for a similar statement concerning the kaon. We have addressed this issue by repeating the analysis described herein for a fictitious $s + \bar{s}$ pseudoscalar bound state. Using a s -quark current mass that produces the empirical ϕ -meson mass [55], we obtain $m_{s\bar{s}0^-} = 0.70 \text{ GeV}$ and find $v_S^{s\bar{s}0^-} = 2.7$ (units of $m_{s\bar{s}0^-}^2$). Interpolating to the kaon mass, we estimate that an off-shell correlation in this channel can serve as a valid meson target on $-t \lesssim 0.9 \text{ GeV}^2$.

ACKNOWLEDGMENTS

We are grateful to R. Ent, T. Horn, G. Huber, C. Keppel, and J. Rodríguez-Quintero for insightful comments. Research supported by Argonne National Laboratory, Office of the Director, through the Named Postdoctoral Fellowship Program; Fundação de Amparo à Pesquisa do Estado de São Paulo - FAPESP Grant No. 2015/21550-4; and U.S. Department of Energy, Office of Science, Office of Nuclear Physics, Contract No. DE-AC02-06CH11357.

-
- [1] E. Fermi and L. Marshall, *Phys. Rev.* **72**, 1139 (1947).
 [2] R. P. Feynman, *Phys. Rev.* **76**, 769 (1949).
 [3] K. D. Lane, *Phys. Rev. D* **10**, 2605 (1974).
 [4] H. D. Politzer, *Nucl. Phys. B* **117**, 397 (1976).
 [5] M. S. Bhagwat, M. A. Pichowsky, C. D. Roberts, and P. C. Tandy, *Phys. Rev. C* **68**, 015203 (2003).
 [6] P. O. Bowman, U. M. Heller, D. B. Leinweber, M. B. Parappilly, A. G. Williams, and J. Zhang, *Phys. Rev. D* **71**, 054507 (2005).
 [7] M. S. Bhagwat and P. C. Tandy, *AIP Conf. Proc.* **842**, 225 (2006).
 [8] J. D. Sullivan, *Phys. Rev. D* **5**, 1732 (1972).
 [9] J. Volmer *et al.*, *Phys. Rev. Lett.* **86**, 1713 (2001).
 [10] T. Horn *et al.*, *Phys. Rev. Lett.* **97**, 192001 (2006).
 [11] V. Tadevosyan *et al.*, *Phys. Rev. C* **75**, 055205 (2007).
 [12] T. Horn *et al.*, *Phys. Rev. C* **78**, 058201 (2008).
 [13] H. P. Blok *et al.*, *Phys. Rev. C* **78**, 045202 (2008).
 [14] R. J. Holt and P. E. Reimer, *AIP Conf. Proc.* **588**, 234 (2001).
 [15] R. J. Holt and C. D. Roberts, *Rev. Mod. Phys.* **82**, 2991 (2010).
 [16] D. Adikaram *et al.*, Measurement of Tagged Deep Inelastic Scattering (TDIS), approved Jefferson Lab experiment E12-15-006 (2015).
 [17] P. Maris, C. D. Roberts, and P. C. Tandy, *Phys. Lett. B* **420**, 267 (1998).
 [18] S. J. Brodsky, C. D. Roberts, R. Shrock, and P. C. Tandy, *Phys. Rev. C* **85**, 065202 (2012).
 [19] N. Nakanishi, *Prog. Theor. Phys. Suppl.* **43**, 1 (1969).
 [20] T. Hatsuda, E. M. Henley, T. Meissner, and G. Krein, *Phys. Rev. C* **49**, 452 (1994).
 [21] H. B. O'Connell, B. C. Pearce, A. W. Thomas, and A. G. Williams, *Prog. Part. Nucl. Phys.* **39**, 201 (1997).
 [22] M. Benayoun, P. David, L. DelBuono, O. Leitner, and H. B. O'Connell, *Eur. Phys. J. C* **55**, 199 (2008).
 [23] K. L. Mitchell and P. C. Tandy, *Phys. Rev. C* **55**, 1477 (1997).
 [24] P. C. Tandy, *Prog. Part. Nucl. Phys.* **39**, 117 (1997).
 [25] P. C. Tandy, Inside Mesons: Coupling Constants and Form-Factors, in Future Directions in Quark Nuclear Physics, Proceedings of the Workshop, Adelaide, Australia, March 10–20, 1998, pp. 62–71.
 [26] B. El-Bennich, G. Krein, L. Chang, C. D. Roberts, and D. J. Wilson, *Phys. Rev. D* **85**, 031502(R) (2012).
 [27] B. El-Bennich, M. A. Paracha, C. D. Roberts, and E. Rojas, *Phys. Rev. D* **95**, 034037 (2017).
 [28] M. R. Frank and C. D. Roberts, *Phys. Rev. C* **53**, 390 (1996).
 [29] M. A. Pichowsky, S. Walawalkar, and S. Capstick, *Phys. Rev. D* **60**, 054030 (1999).
 [30] S. R. Cotanch and P. Maris, *Phys. Rev. D* **66**, 116010 (2002).
 [31] S. R. Cotanch and P. Maris, *Phys. Rev. D* **68**, 036006 (2003).
 [32] M. S. Bhagwat *et al.*, *Few-Body Syst.* **40**, 209 (2007).
 [33] L. Chang and C. D. Roberts, *Phys. Rev. C* **85**, 052201(R) (2012).
 [34] B. El-Bennich, G. Krein, E. Rojas, and F. E. Serna, *Few-Body Syst.* **57**, 955 (2016).
 [35] S.-x. Qin, *Few-Body Syst.* **57**, 1059 (2016).
 [36] K. Raya, M. Ding, A. Bashir, L. Chang, and C. D. Roberts, *Phys. Rev. D* **95**, 074014 (2017).
 [37] G. Eichmann, C. S. Fischer, and H. Sanchis-Alepuz, *Phys. Rev. D* **94**, 094033 (2016).
 [38] P. Maris and C. D. Roberts, *Int. J. Mod. Phys. E* **12**, 297 (2003).
 [39] C. D. Roberts, *J. Phys. Conf. Ser.* **706**, 022003 (2016).
 [40] T. Horn and C. D. Roberts, *J. Phys. G* **43**, 073001 (2016).
 [41] G. Eichmann, H. Sanchis-Alepuz, R. Williams, R. Alkofer, and C. S. Fischer, *Prog. Part. Nucl. Phys.* **91**, 1 (2016).
 [42] H. J. Munczek, *Phys. Rev. D* **52**, 4736 (1995).
 [43] A. Bender, C. D. Roberts, and L. von Smekal, *Phys. Lett. B* **380**, 7 (1996).

- [44] D. Binosi, L. Chang, J. Papavassiliou, S.-X. Qin, and C. D. Roberts, *Phys. Rev. D* **93**, 096010 (2016).
- [45] L. Chang and C. D. Roberts, *Phys. Rev. Lett.* **103**, 081601 (2009).
- [46] D. Binosi, L. Chang, J. Papavassiliou, and C. D. Roberts, *Phys. Lett. B* **742**, 183 (2015).
- [47] D. Binosi, *EPJ Web Conf.* **113**, 05002 (2016).
- [48] D. Binosi, C. Mezrag, J. Papavassiliou, C. D. Roberts, and J. Rodriguez-Quintero, *Phys. Rev. D* **96**, 054026 (2017).
- [49] L. Chang, I. C. Cloet, J. J. Cobos-Martinez, C. D. Roberts, S. M. Schmidt, and P. C. Tandy, *Phys. Rev. Lett.* **110**, 132001 (2013).
- [50] J. Segovia *et al.*, *Phys. Lett. B* **731**, 13 (2014).
- [51] C. Shi, C. Chen, L. Chang, C. D. Roberts, S. M. Schmidt, and H. S. Zong, *Phys. Rev. D* **92**, 014035 (2015).
- [52] P. Maris and C. D. Roberts, *Phys. Rev. C* **56**, 3369 (1997).
- [53] J. C. R. Bloch, *Phys. Rev. D* **66**, 034032 (2002).
- [54] S.-X. Qin, L. Chang, Y.-X. Liu, C. D. Roberts, and D. J. Wilson, *Phys. Rev. C* **84**, 042202(R) (2011).
- [55] S.-X. Qin, L. Chang, Y.-X. Liu, C. D. Roberts, and D. J. Wilson, *Phys. Rev. C* **85**, 035202 (2012).
- [56] P. Maris and P. C. Tandy, *Phys. Rev. C* **60**, 055214 (1999).
- [57] C. Patrignani *et al.* (Particle Data Group), *Chin. Phys. C* **40**, 100001 (2016).
- [58] K. Langfeld, H. Markum, R. Pullirsch, C. D. Roberts, and S. M. Schmidt, *Phys. Rev. C* **67**, 065206 (2003).
- [59] P. Maris and P. C. Tandy, *Phys. Rev. C* **62**, 055204 (2000).
- [60] L. Chang, I. C. Cloët, C. D. Roberts, S. M. Schmidt, and P. C. Tandy, *Phys. Rev. Lett.* **111**, 141802 (2013).
- [61] P. Maris and C. D. Roberts, *Phys. Rev. C* **58**, 3659 (1998).
- [62] G. P. Lepage and S. J. Brodsky, *Phys. Lett. B* **87**, 359 (1979).
- [63] G. P. Lepage and S. J. Brodsky, *Phys. Rev. D* **22**, 2157 (1980).
- [64] A. V. Efremov and A. V. Radyushkin, *Phys. Lett. B* **94**, 245 (1980).
- [65] J.-H. Zhang, J.-W. Chen, X. Ji, L. Jin, and H.-W. Lin, *Phys. Rev. D* **95**, 094514 (2017).
- [66] K. Raya, L. Chang, A. Bashir, J. J. Cobos-Martinez, L. X. Gutierrez-Guerrero, C. D. Roberts, and P. C. Tandy, *Phys. Rev. D* **93**, 074017 (2016).
- [67] X.-D. Ji, *Phys. Rev. D* **55**, 7114 (1997).
- [68] A. V. Radyushkin, *Phys. Rev. D* **56**, 5524 (1997).
- [69] D. Mueller, D. Robaschik, B. Geyer, F. M. Dittes, and J. Hořejši, *Fortschr. Phys.* **42**, 101 (1994).
- [70] F. Yuan, *Phys. Rev. D* **69**, 051501 (2004).
- [71] C. Mezrag *et al.*, *Phys. Lett. B* **741**, 190 (2015).